

# Optical frequency comb assisted laser system for multiplex precision spectroscopy

L. Consolino,<sup>1,\*</sup> G. Giusfredi,<sup>1,2</sup> P. De Natale,<sup>1,2</sup> M. Inguscio,<sup>1</sup>  
and P. Cancio<sup>1,2</sup>

<sup>1</sup>European Laboratory for Non-Linear Spectroscopy (LENS) and Dipartimento di Fisica,  
Università degli Studi di Firenze, Via N. Carrara 1, 50019 - Sesto Fiorentino (FI) - Italy

<sup>2</sup>Istituto Nazionale di Ottica - Consiglio Nazionale delle Ricerche (INO-CNR), Largo E. Fermi  
6, 50125 - Firenze - Italy

[\\*consolino@lens.unifi.it](mailto:consolino@lens.unifi.it)

**Abstract:** A laser system composed of two lasers phase-locked onto an Optical Frequency Comb Synthesizer (OFCS), operating around 1083 nm, was developed. An absolute frequency precision of  $6 \times 10^{-13}$  at 1s, limited by the OFCS, was measured with a residual rms phase-noise of 71 mrad and 87 mrad for the two phase-locks, respectively. Multiplex spectroscopy on 1083 nm Helium transitions with this set-up is demonstrated. Generalization of this system to a larger number of OFCS assisted laser sources for wider frequency separations, even in other spectral regions, is discussed.

© 2011 Optical Society of America

**OCIS codes:** (300.6210) Spectroscopy, atomic; (300.6320) Spectroscopy, high-resolution; Optical frequency synthesizer.

---

## References and links

1. J. Reichert, R. Holzwarth, T. Udem, and T. W. Hansch, "Measuring the frequency of light with mode-locked lasers," *Opt. Commun.* **172**, 5968 (1999).
2. T. Udem, R. Holzwarth, and T. W. Hansch, "Optical frequency metrology," *Nature* **416**, 233240 (2002).
3. P. Maddaloni, P. Cancio Pastor, and P. De Natale, "Optical comb generators for laser frequency measurement," *Meas. Sci. Technol.* **20**, 052001 (2009).
4. V. Gerginov, C. E. Tanner, S. A. Diddams, A. Bartels, and L. Hollberg, "High-resolution spectroscopy with a femtosecond laser frequency comb," *Opt. Lett.* **30** 17346 (2005).
5. M. J. Thorpe, K. D. Moll, R. J. Jones, B. Safdi B, and J. Ye, "Broadband cavity ringdown spectroscopy for sensitive and rapid molecular detection," *Science* **311** 15959 (2006).
6. G. Giusfredi, P. De Natale, D. Mazzotti, P. Cancio Pastor, C. de Mauro, L. Fallani, G. Hagel, V. Krachmalnicoff, and M. Inguscio, "Present status of the fine structure frequencies of the  $2^3P$  Helium level," *Can. J. Phys.* **83**(4), 301–310 (2005).
7. T. Zelevinsky, D. Farkas, and G. Gabrielse, "Precision Measurement of the Three  $2^3P_j$  Helium Fine Structure Intervals," *Phys. Rev. Lett.* **95**, 203001 (2005).
8. J. S. Borbely, M. C. George, L. D. Lombardi, M. Weel, D. W. Fitzakerley, and E. A. Hessels, "Separated oscillatory-field microwave measurement of the  $2^3P_1 2^3P_2$  fine-structure interval of atomic helium," *Phys. Rev. A* **79**, 060503 (2009).
9. M. Smiciklas and D. Shiner, "Determination of the Fine Structure constant using Helium Fine Structure," *Phys. Rev. Lett.* **104**, 070403 (2010).
10. K. Pachucki and V. A. Yerokhin, "Fine Structure of Heliumlike Ions and Determination of the Fine Structure Constant," *Phys. Rev. Lett.* **104**, 070403 (2010).
11. J. D. Prestage, C. E. Johnson, E. A. Hinds, and F. M. J. Pichanick, "Precise study of hyperfine structure in the  $2^3P$  state of  $^3\text{He}$ ," *Phys. Rev. A* **32**, 2712–2724 (1985).
12. D. C. Morton, Q. X. Wu, and G. W. F. Drake, "Energy levels for the stable isotopes of atomic helium (He-4 I and He-3 I)," *Can. J. Phys.* **84**, 83–105 (2006).

13. D. Shiner, R. Dixon, and V. Vedantham, "Three-Nucleon Charge Radius: A Precise Laser Determination Using  $^3\text{He}$ ," *Phys. Rev. Lett.* **74**, 3553–3556 (1995).
14. D. C. Morton, Q. Wu, and G. W. F. Drake, "Nuclear charge radius for  $^3\text{He}$ ," *Phys. Rev. A* **73**, 034502 (2006).
15. P. Cancio Pastor, G. Giusfredi, P. De Natale, G. Hagel, C. de Mauro, and M. Inguscio, "Absolute Frequency Measurements of the  $2^3\text{S}_1 \rightarrow 2^3\text{P}_{0,1,2}$  Atomic Helium Transitions around 1083 nm," *Phys. Rev. Lett.* **92**, 023001 (2004).
16. P. Cancio Pastor, G. Giusfredi, P. De Natale, G. Hagel, C. de Mauro, and M. Inguscio, "Absolute Frequency Measurements of the  $2^3\text{S}_1 \rightarrow 2^3\text{P}_{0,1,2}$  Atomic Helium Transitions around 1083 nm: erratum," *Phys. Rev. Lett.* **97**, 139903 (2006).
17. V. A. Yerokhin and K. Pachucki, "Theoretical energies of low-lying states of light helium-like ions," *Phys. Rev. A* **81**, 022507 (2010).
18. M. Prevedelli, P. Cancio, G. Giusfredi, F. S. Pavone, and M. Inguscio, "Frequency control of DBR diode lasers at 1.08 micrometer and precision spectroscopy of Helium," *Opt. Commun.* **125**, 231 (1996).
19. I. Galli, S. Bartalini, P. Cancio, G. Giusfredi, D. Mazzotti, and P. De Natale, "Ultra-stable, widely tunable and absolutely linked mid-IR coherent source," *Opt. Express* **17**, 9583–9587 (2009).
20. K. Döringshoff, I. Ernsting, R.-H. Rinkleff, S. Schiller, and A. Wicht, "Frequency comb-referenced narrow line width diode laser system for coherent molecular spectroscopy," *Appl. Phys. B* **91**, 4956 (2008).
21. L. Cacciapuoti, M. de Angelis, M. Fattori, G. Lamporesi, T. Petelski, M. Prevedelli, J. Stuhler, and G. M. Tino, "Analog+digital phase and frequency detector for phase locking of diode lasers," *Rev. Sci. Instrum.* **76**, 053111 (2005).

## 1. Introduction

After one decade since its discovery [1], the uniqueness of the Optical Frequency Comb Synthesizers (OFCS) for precision spectroscopy is well established (see [2, 3] for a recent review). Besides enabling accurate frequency measurements of atomic and molecular transitions in the UV/optical/IR spectral regions, OFCS's are also spectroscopic sources, providing excellent accuracy, high spectral purity and broad spectral coverage. Recently, multiplex atomic and molecular spectroscopy has been allowed by using directly an OFCS as resonant laser source [4, 5]. Accurate frequency differences between transitions of the same or different atomic/molecular species can be simultaneously measured by using such direct OFCS spectroscopy (DFCS). However, for experiments where small frequency differences or slight frequency variations must be measured, some inaccuracies can appear, due to systematic errors induced by the non-resonant comb light. In this paper, we present an alternative quasi-multiplex technique that uses two (or more) OFCS-phase-locked laser sources which are resonant with two (or more) different atomic/molecular transitions, keeping both the benefits of the OFCS and of the high precision cw laser spectroscopy technique. We test this system on frequency measurements of atomic Helium transitions around 1083 nm wavelength.

High precision Helium spectroscopy has become, since the beginning of the 80s, a very important tool for fundamental physics. In this framework, accurate measurements of the fine structure (FS) splittings of the lowest triplet P level ( $2^3P$ ) of the stable Helium boson ( $^4\text{He}$ ) were preferred to FS frequencies of simpler atomic systems, namely Hydrogen, to get a few ppb determination of the fine structure constant  $\alpha$  by atomic spectroscopy [6–10]. Moreover, frequency measurements of the  $2^3P$  hyperfine (HFS) splittings in the stable He fermion ( $^3\text{He}$ ) give information about the strong nuclear interaction in this atom [11, 12]. The isotope shift (IS) contribution due to the finite nuclear volume is determined by measuring frequency differences between transitions of different He isotopes, hence by an atomic physics determination of the nuclear charge radius of He isotopes [13, 14]. In addition, high precision frequency measurements of atomic transitions can be a useful test for frontier theoretical calculations, like Quantum Electro-Dynamics (QED) energy contributions for simple bounded systems, as Helium [12, 15–17]. Multi-resonant precision spectroscopy of the  $2^3\text{S} \rightarrow 2^3\text{P}$  He transitions by using the system described here allows at the same time measurements of the absolute frequencies around 1083 nm and of the FS, HFS and IS microwave splittings at the same accuracy level. Such experimental approach can be easily extended to a large number of OFCS phase-locked

laser sources and implemented in other spectral regions.

## 2. Laser system setup

A detailed scheme of the experimental setup is shown in Fig. 1. Two different 1083 nm *Distributed Bragg Reflector* (DBR) diode laser sources, resonant with different He transitions, are phase-locked to a near-IR OFCS. This OFCS is a commercial system from Menlo, based on an amplified fs fiber laser with an octave spectral coverage from 1 to 2  $\mu\text{m}$ , at 100 MHz repetition rate ( $f_r$ ). Both carrier-envelope offset frequency ( $f_0$ ) and  $f_r$  are frequency referenced to a 10 MHz quartz-clock with a stability of  $6 \times 10^{-13}$ . The quartz is directly traceable against the primary frequency standard by using a Rb-GPS clock system with an accuracy better than  $10^{-12}$ . For each diode laser, the emission is single mode at room temperature, with a maximum power of about 50 mW @ I=180 mA. The diodes are narrowed down to 300 kHz FWHM linewidth by using an external cavity configuration [18]. The lasers frequencies are controlled against a near-IR OFCS by using the scheme described as follows. The first laser (L1) is directly phase-locked to the nearest OFCS tooth  $N_1$ , by beating both on a fast photodetector. Phase fluctuations of the cw laser with respect to the comb are corrected by analyzing the detected beatnote,  $f_{c1}$ , using a fast optical phase-locked loop correction circuit (OPLL1), which uses a 30 MHz synthesized frequency as a local oscillator,  $f_{LO}$ . For the second laser (L2), two

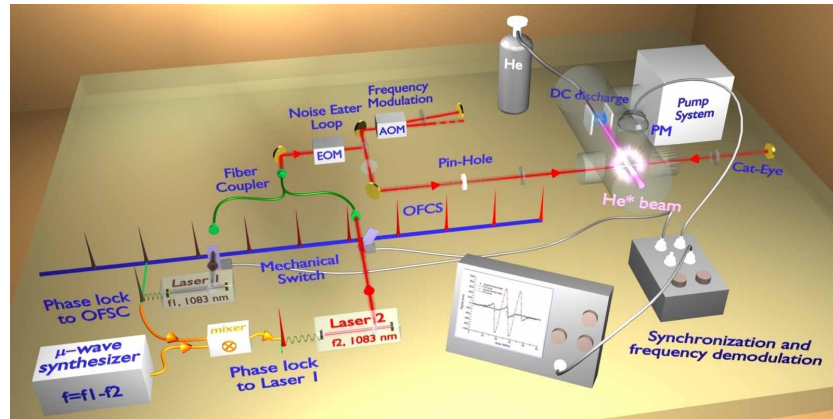


Fig. 1. Experimental set-up.

approaches can be followed. The first one is just to replicate the phase-lock loop also for the other laser, by beating it with the nearest OFCS tooth. The second approach is based on a direct phase-lock between the two diode lasers. In the latter approach, all excess OFCS phase-noise is avoided, obtaining, in principle, two identical diode lasers. We followed this approach because it guarantees that the two lasers emit at different frequencies, but with the same spectral characteristics, as required by multiplex precision spectroscopy. The phase-correction signal, in this case, is recorded by directly beating both cw laser on a fast photodetector, at laser separations of tens of GHz, as in the case of He transitions at 1083 nm. For larger separations, the OFCS can be used as an optical frequency mixer to compare and control directly the phase/frequency noise of the two cw lasers, as we have demonstrated for laser sources more than 70 THz apart [19]. A second OPLL circuit (OPLL2) is used for the phase-lock of the two diode lasers. The detected beat-note,  $f_{12}$  is frequency down converted to  $f_{LO}$  by mixing it with a microwave synthesized frequency,  $f_{\mu w}$ . In this way, we have developed a GPS traceable absolute frequency chain for

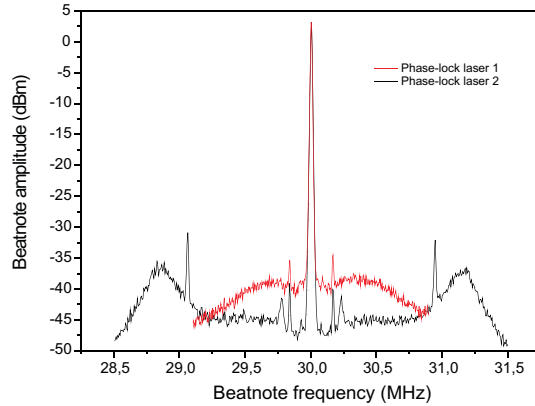


Fig. 2. Phase-lock beatnote for the OPLL1 (red) and OPLL2 (black) loops.

both lasers given by:

$$f_1 = f_0 + N_1 f_r + f_{c1} = f_0 + N_1 f_r + f_{LO} \quad (1)$$

$$f_2 = f_1 + f_{12} = f_0 + N_1 f_r + f_{\mu w} + f_{LO} \quad (2)$$

Moreover, simultaneous synthesized scans of both frequencies are allowed by changing the  $f_r$  frequency. Alternatively, the frequency difference between both lasers is scanned by changing  $f_{\mu w}$ . Both OPLL1 and OPLL2 circuits are hybrid analogical/digital comparators to maximize phase sensitivity and dynamic range. In Fig. 2, the phase-locked beat notes for both lasers (OPLL1 in red and OPLL2 in black) are shown. From the servo-bumps in these figures, phase-lock bandwidths of 500 kHz and 1.2 MHz were measured for OPLL1 and OPLL2, respectively. The OPLLs performance in terms of residual rms phase-error is measured by using the fractional power  $\eta$  contained in the coherent part of the beatnote signal, i.e. in the carrier. The ratio between the rf power in the carrier beatnote peak and the total rf power including noise within a certain integration bandwidth gives the  $\eta$  value for each OPLL. We have measured  $\eta_{OPLL1}=99.5\%$  and  $\eta_{OPLL2}=99.2\%$  by considering the beatnote spectra shown in Fig. 2 and bandwidths of 2 MHz and 3 MHz, respectively. Due to  $\eta = e^{(-\phi_{rms}^2)}$ , we measured a residual rms phase-noise of 71 mrad and 88 mrad for OPLL1 and OPLL2, respectively. These values are of the same order as others measured for similar optical phase-locked loops used in precision spectroscopy and metrological applications [20, 21]. In fact, they guarantee the same spectral characteristics, i.e linewidth, for the phase-locked sources. Following the frequency chain of our system, L2 has the same linewidth of L1, and L1 the same as the OFCS, which is about 50 kHz for wavelengths around 1  $\mu\text{m}$ . Equally important for precision spectroscopy applications is to characterize the absolute frequency precision and accuracy of each laser. First, we have measured the frequency stability in the time domain by means of Allan variance. The beat note frequencies at 30 MHz for both OPLL1 and OPLL2 loops were counted at a 100 ms rate when the lasers were phase-locked. We have calculated the Allan variance from these counts, as shown in Fig. 3. In both cases, a  $1/\tau$  trend was measured with values 28 mHz and 10 mHz at 1 s for OPLL1 and OPLL2, respectively. In these conditions, frequency stability is dominated by white noise, at least in the 200 s time scale, and both lasers have the same frequency stability of the OFCS. It means a precision of  $6 \cdot 10^{-13}$  in 1 s for both  $f_1$  and  $f_2$  frequencies and an accuracy of 300 Hz at 1083 nm. We remark that both precision and accuracy can be improved by using an OFCS master oscillator with better performances than the Rb-GPS disciplined quartz-oscillator used by our OFCS.

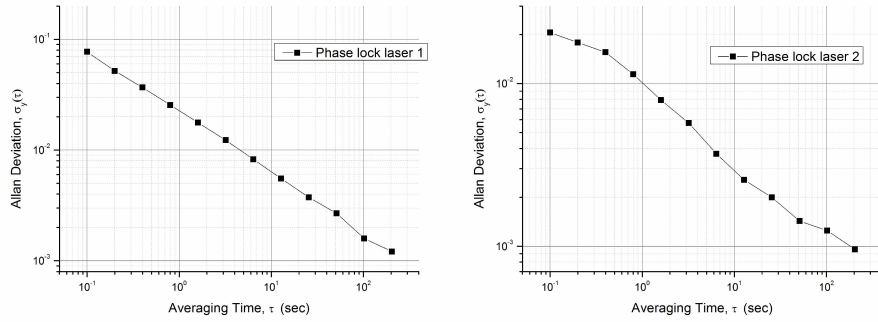


Fig. 3. Allan variance of the OPLL1 and OPLL2. On the left laser1 is locked to the nearest comb tooth. On the right, laser2 is locked to laser1. Vertical axes in Hz.

### 3. Application to multiplex precision Helium spectroscopy

In order to test the performance and capabilities of this laser system in precise frequency measurements, sub-Doppler spectroscopy on metastable He atoms at 1083 nm was realized. The atoms, metastabilized by using a continuous high voltage discharge on a collimated He beam, interact at right angle with the forward-backward radiation from the diode lasers, as shown in Fig. 1. Saturated fluorescence from the  $2^3P$  excited state is detected while the laser fre-

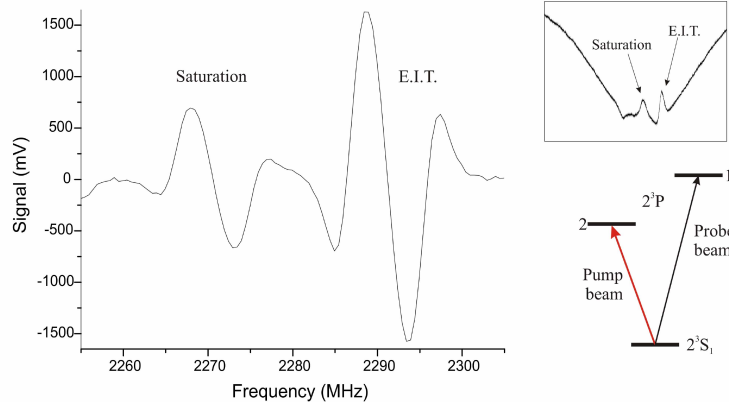


Fig. 4. EIT spectrum for the V coherence spectroscopy configuration with L1 resonant with  $^4\text{He } 2^3S_1 \rightarrow 2^3P_2$  transition and L2 resonant with  $^4\text{He } 2^3S_1 \rightarrow 2^3P_1$  one, when the L2 frequency is scanned and L1 frequency is fixed. Saturation dip spectrum due to L2 is also shown.

quencies are scanned. Laser frequency modulation and third-derivative lock-in detection allow to increase the S/N ratio of the detected fluorescence saturation dips, and hence the precision in line center measurements. Details about the He spectrometer are given elsewhere [6, 15, 16]. In the present context, it is important to preserve the same optical configuration for all the laser sources interacting with atoms, avoiding different systematic effects for each one. Optical fiber coupling of both diode lasers matches this requirement. In this way, a common optical path

after the fiber coupler is fixed, including AOM frequency modulation for third derivative detection. The AOM modulator operates around 110 MHz, and is mounted in double pass, which shifts down of 220 MHz the laser frequencies of Eqs. (1) and (2), with respect to the He transitions. A noise-eater and cat's-eye back-reflecting systems, both placed in the common optical path after the fiber coupler, guarantee the same interacting laser power and saturation alignment for both lasers. In Fig. 4, we show a spectrum that contains some of the possible features which can be observed with this laser system. In this case, L1 and L2 are resonant with the  ${}^4\text{He}$   $2^3S_1 \rightarrow 2^3P_2$  ( $f_{P_2}$ ) and  $2^3S_1 \rightarrow 2^3P_1$  ( $f_{P_1}$ ) transitions, respectively, in a typical V coherence spectroscopy configuration. The L1 frequency is fixed while the L2 frequency is scanned around the  $f_{P_1}$  frequency. The X-axis scale in this figure is given in terms of  $f_{P_2}-f_{P_1}$  difference to show that the EIT signal is centered at this difference, independently of the laser frequency with respect to the  $f_{P_2}$  and  $f_{P_1}$  He frequencies. This shows another potential use of this system: a controlled synthesized detuning between both sources in applications that use Raman or coherent spectroscopy configurations. The other signal shown in Fig. 4 is the  $f_{P_1}$  saturation dip. Although we have depicted it in the same frequency scale as the EIT signal, this signal is centered at the optical frequencies of L2. The frequency difference between the  $f_{P_1}$  dip and the EIT signal in this figure is just the OFCS controllable detuning of L1 with respect to L2, i.e. 20 MHz in this case.

Precision and reproducibility of He transition frequencies have been checked by measuring the same transition with both lasers in the configuration shown in Fig. 5. In this case, both lasers are resonant with the  ${}^4\text{He}$   $2^3S_1 \rightarrow 2^3P_1$  transition with a 10 MHz frequency shift between  $f_1$  and  $f_2$ , in order to distinguish the contribution from L1 and L2, respectively. In addition, to avoid systematic effects due to laser radiation resonant with one transition into the other, only one laser at a time shed onto the sample, the other being blocked. Two mechanical switches, introduced in the laser paths before common fiber coupling, are used for periodic blocking, with a 1 s period. During this acquisition time, density and velocity of interacting metastable He atoms are constant, and hence the two quasi-simultaneous He spectra are recorded in the same experimental conditions. The He fluorescence signals are detected by a phototube while

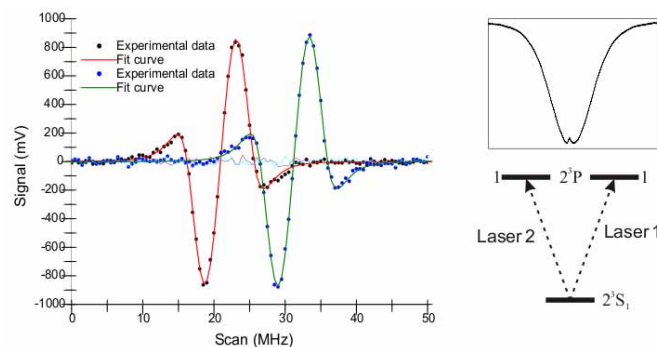


Fig. 5. Saturated fluorescence of the  $2^3S_1 \rightarrow 2^3P_1$  transition of  ${}^4\text{He}$ . On the right, the laser configuration (both lasers on the same line) and the fluorescence dip on top of the residual Gaussian shape, for one resonant laser, are shown. On the left, the recorded third derivative lineshape of the saturation dips, with fitting curves, are shown. The two signals should be overlapped, but they have been shifted for the sake of clarity. Acquisition parameters were 40 MHz OFCS scanwidth, 100 points for each spectrum, using a lock-in integration time of 700 ms for each point.

the OFCS frequency  $f_r$  is scanned. They have Gaussian profile, with 80 MHz HWHM. A saturation dip is visible in the center, as shown in Fig. 5 for one interacting laser. Third derivative

spectra of saturation dips are shown, when the OFCS is scanned about 40 MHz around the dip center, together with the fits to a third derivative of a Lorentzian shape. Typical precisions between 5-25 kHz in the dip center determination are obtained, depending on the S/N ratio. We have performed several runs of measurements with different laser relocks. The results are shown in Fig. 6. On the left, we show the statistical distribution of the absolute frequency,  $f_{P_1}$ , measured by using each OFCS-referenced laser, i.e.  $f_{P_1}^1$  and  $f_{P_1}^2$ . In both cases, a kHz precision (i.e.  $\Delta f/f = 4 \times 10^{-12}$ ) is achieved by weighted averaging a few tens of measurements, which is limited by the 3.2 MHz FWHM He transition linewidth, not by the laser system. In addition, the frequency difference between two averaged values is compatible with zero with a 1 kHz error bar, confirming that both lasers have the same spectral characteristics. We have done a crossed check of this feature by calculating the difference of the absolute frequencies for each measurement run, i.e.  $f_{P_1}^{12} = f_{P_1}^1 - f_{P_1}^2$ . The results are shown in the right graph of Fig. 6. Also in this case a Gaussian statistical distribution of differences is observed with zero weighted-mean with 1 kHz uncertainty. A frequency reproducibility at the precision level is also confirmed for the differences. As expected, the common interaction optical path for both lasers guarantees the same uncertainty sources for both measured He frequencies. Therefore, this multiplex laser system proves to be well suited simultaneously measuring absolute frequencies of 1083 nm He transitions and FS, HFS and IS splittings at the same precision level.

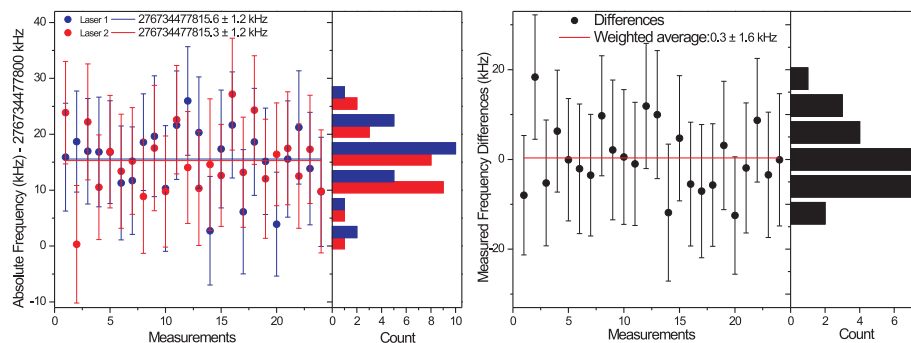


Fig. 6. On the left, statistical distribution of 25 run of measurements when both lasers are resonant with the  $^4\text{He } 2^3S_1 \rightarrow 2^3P_1$  transition. The weighted-mean value for both lasers is also shown. On the right, statistical distribution and weighted-mean of the point-to-point frequency differences of the measurements shown in the left graph.

#### 4. Conclusion

In conclusion, we have developed a OFCS-linked frequency chain of two diode laser sources at 1083 nm with frequency separations up to tens of GHz. The spectral purity of such laser sources is limited by the OFCS one, due to the use of large bandwidth phase-lock loops. Such laser system can be applied for multiplex precision spectroscopy where systematic effects due to non resonant light must be avoided, as we have demonstrated for He transitions around 1083 nm. Moreover, in this case, simultaneous absolute frequencies of optical transitions and frequency differences between them can be measured at the same level of precision. The number of OFCS assisted laser sources can be easily increased, even in other spectral regions, and with larger frequency separations between them. Such systems are proposed for applications that require a precise coherent manipulation of individual atomic or molecular quantum states, and, in general, for phase locking to a low-power optical reference under noisy conditions.

## **Acknowledgments**

This work was partially funded by CNR and the other European research funding Agencies participating to the European Science Foundation EUROCORES Program EUROQUAM-CIGMA, and by Ente Cassa di Risparmio di Firenze.